



# Introduction to Nanotechnology and Nanoscience – Class#9

*Liwei Lin*

Professor, Dept. of Mechanical Engineering  
Co-Director, Berkeley Sensor and Actuator Center  
The University of California, Berkeley, CA94720

e-mail: [lwlin@me.berkeley.edu](mailto:lwlin@me.berkeley.edu)

<http://www.me.berkeley.edu/~lwlin>



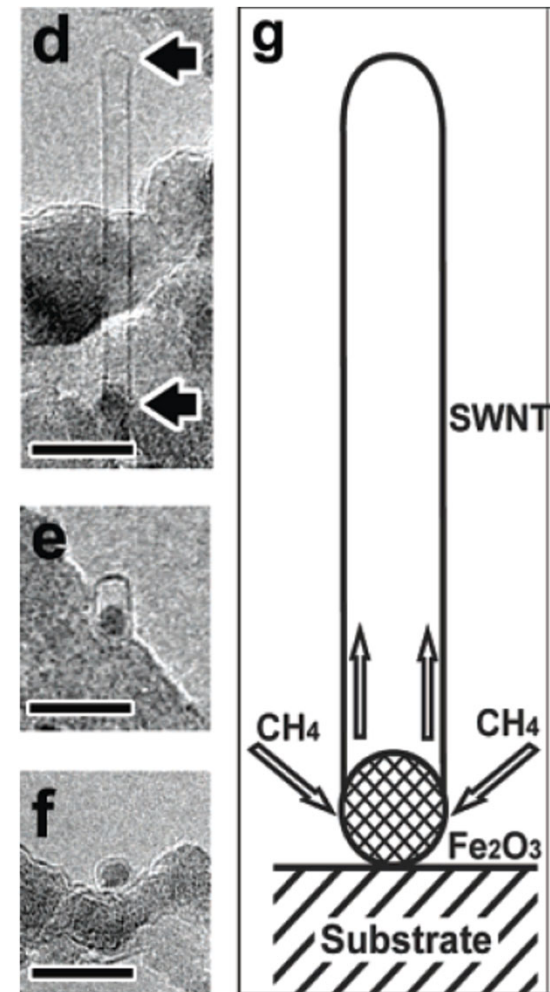
# Outline

- Recap on Class#8
- CNT (n,m)
- CNT Applications
- Paper #2 final parts
- Lab #1



# Growth Condition

- Substrate
  - Silicon dioxide (why not silicon?)
  - Other oxides
  - Metal
- Catalyst Particle
  - Determine the diameter of CNT
  - Evaporation
  - Solution
- Gas
- Temperature

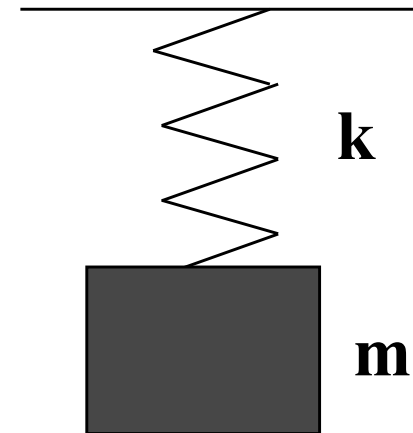




# Resonator Frequency

- Resonator Frequency: spring-mass

$$f = \frac{1}{2\pi} \sqrt{\frac{k}{m}}$$



- Clamped-Clamped beam

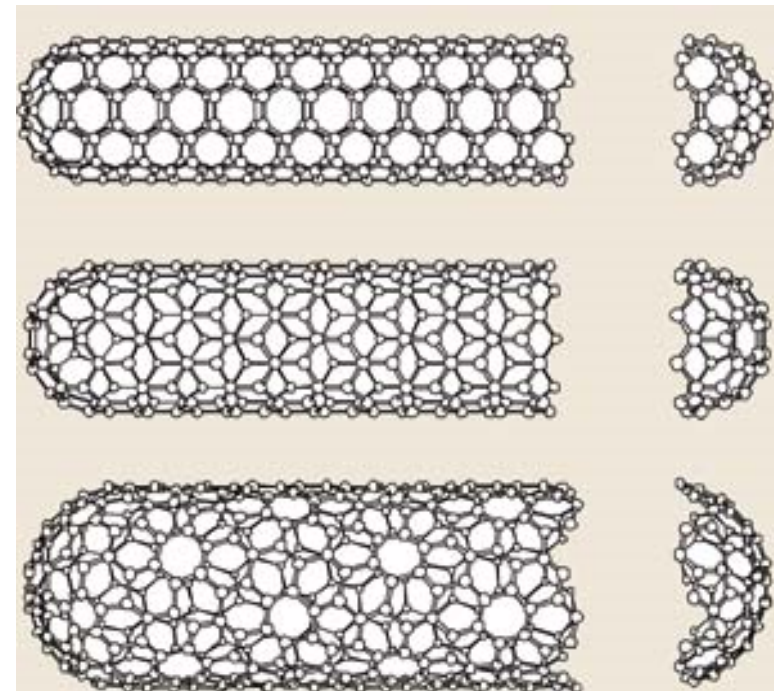
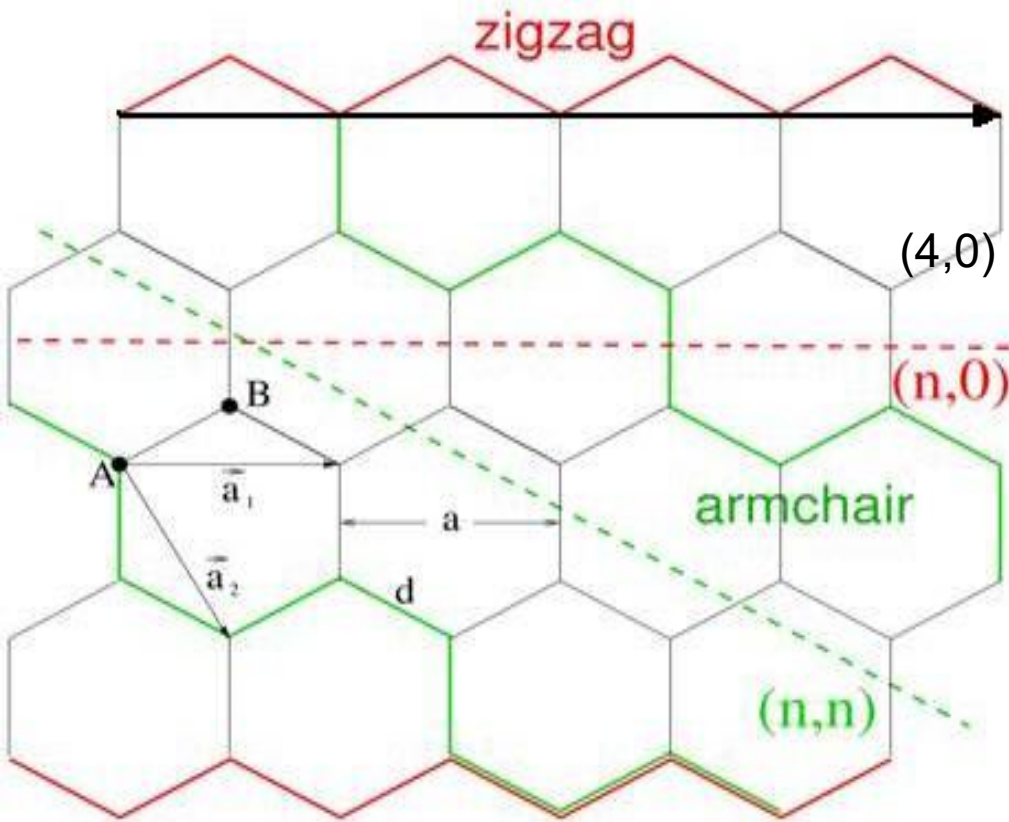
$$k = \frac{192EI}{L^3}$$





# Physical Structure of SWNTs

$a_1$  and  $a_2$  are the unit cell base vectors



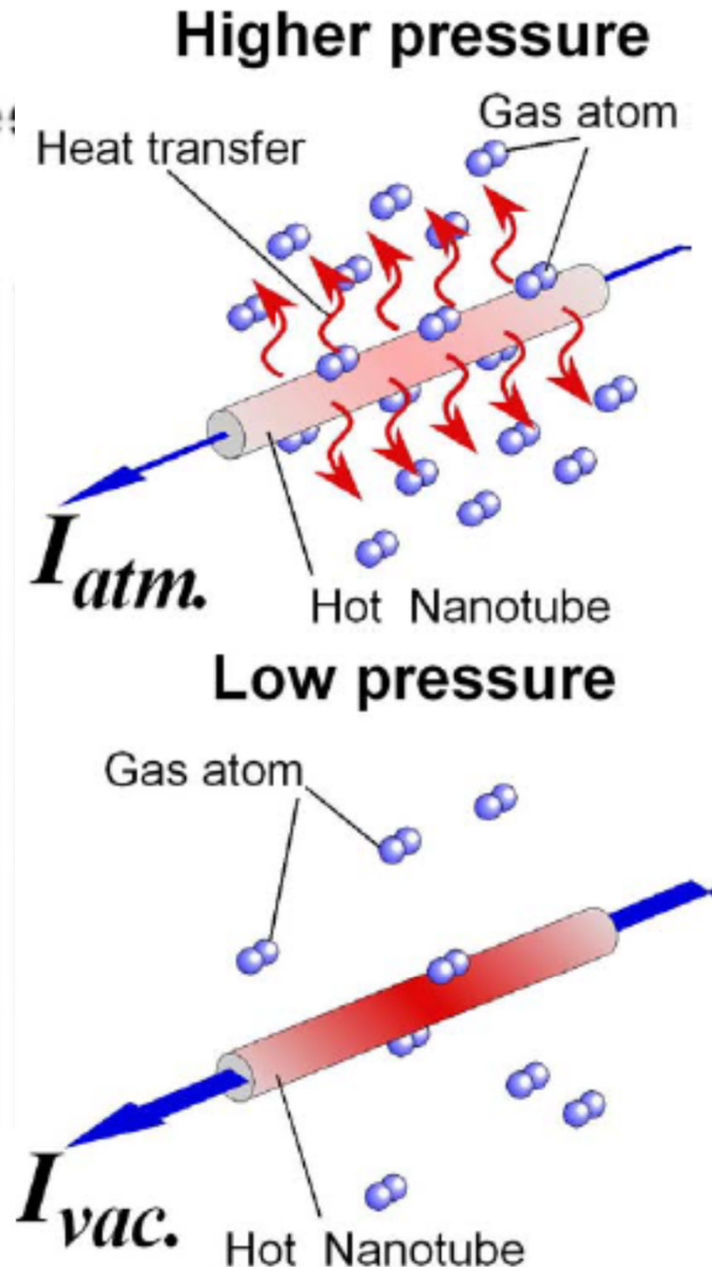
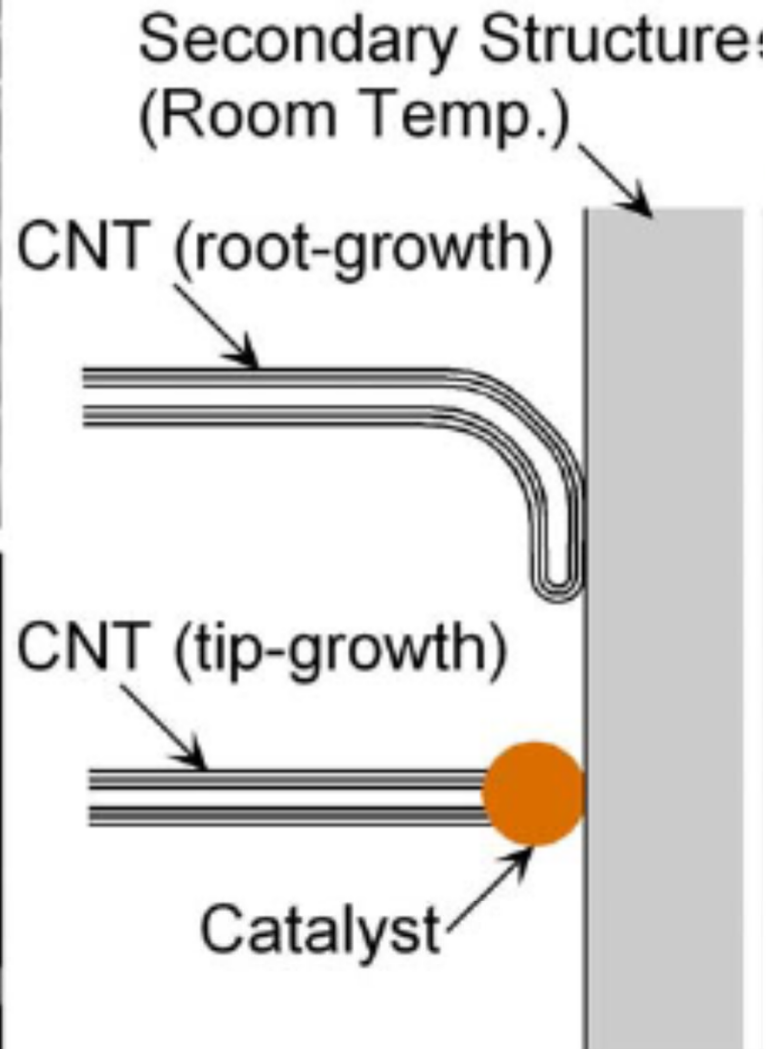
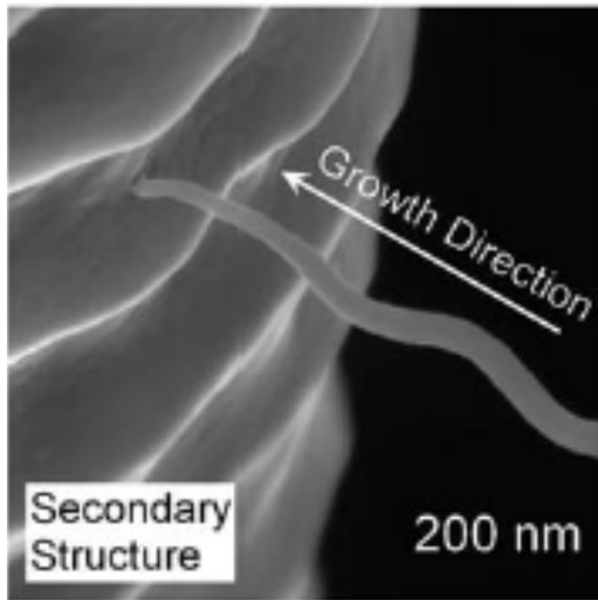
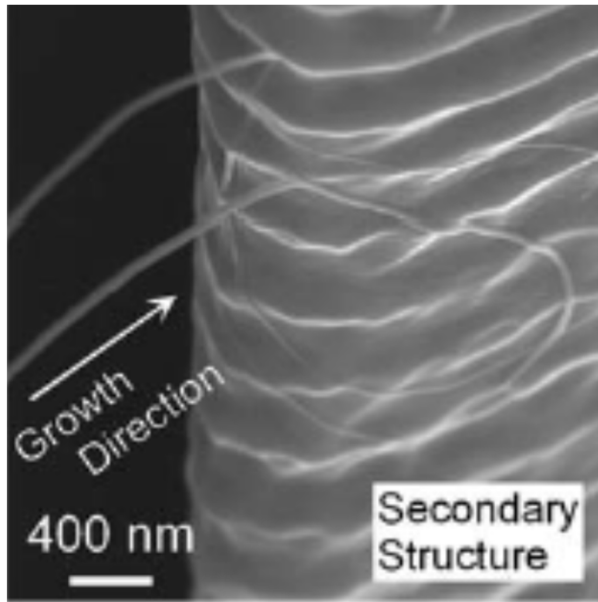
$(n,n)$   
armchair

$(n,0)$   
zig-zag

chiral

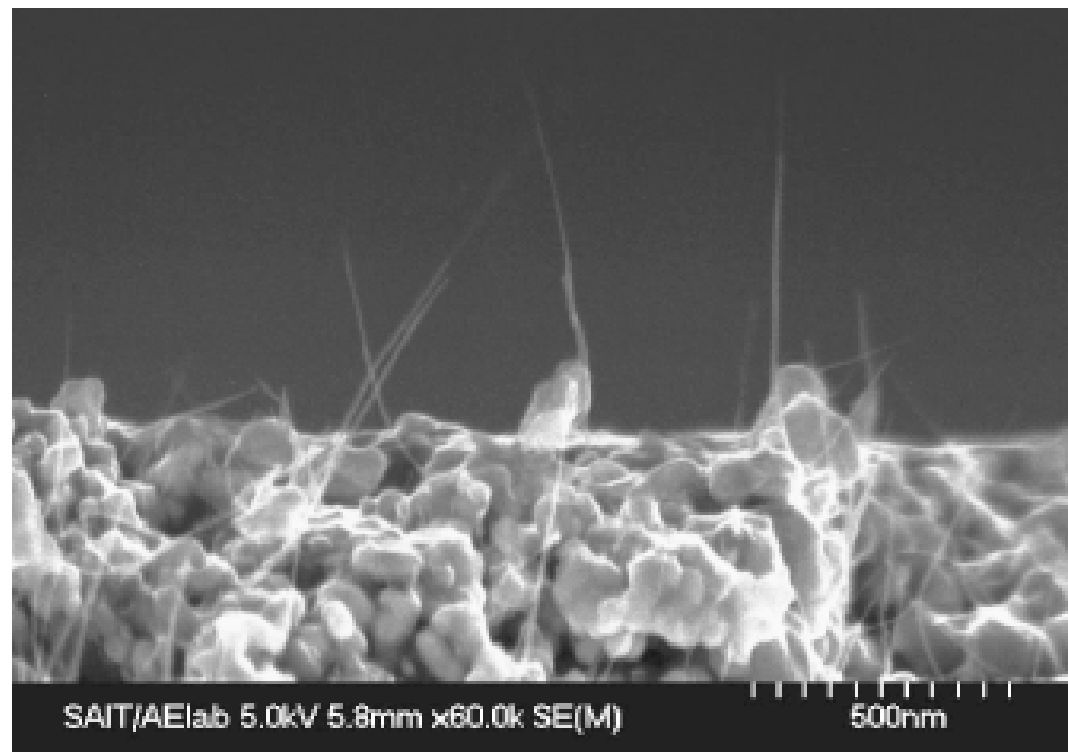
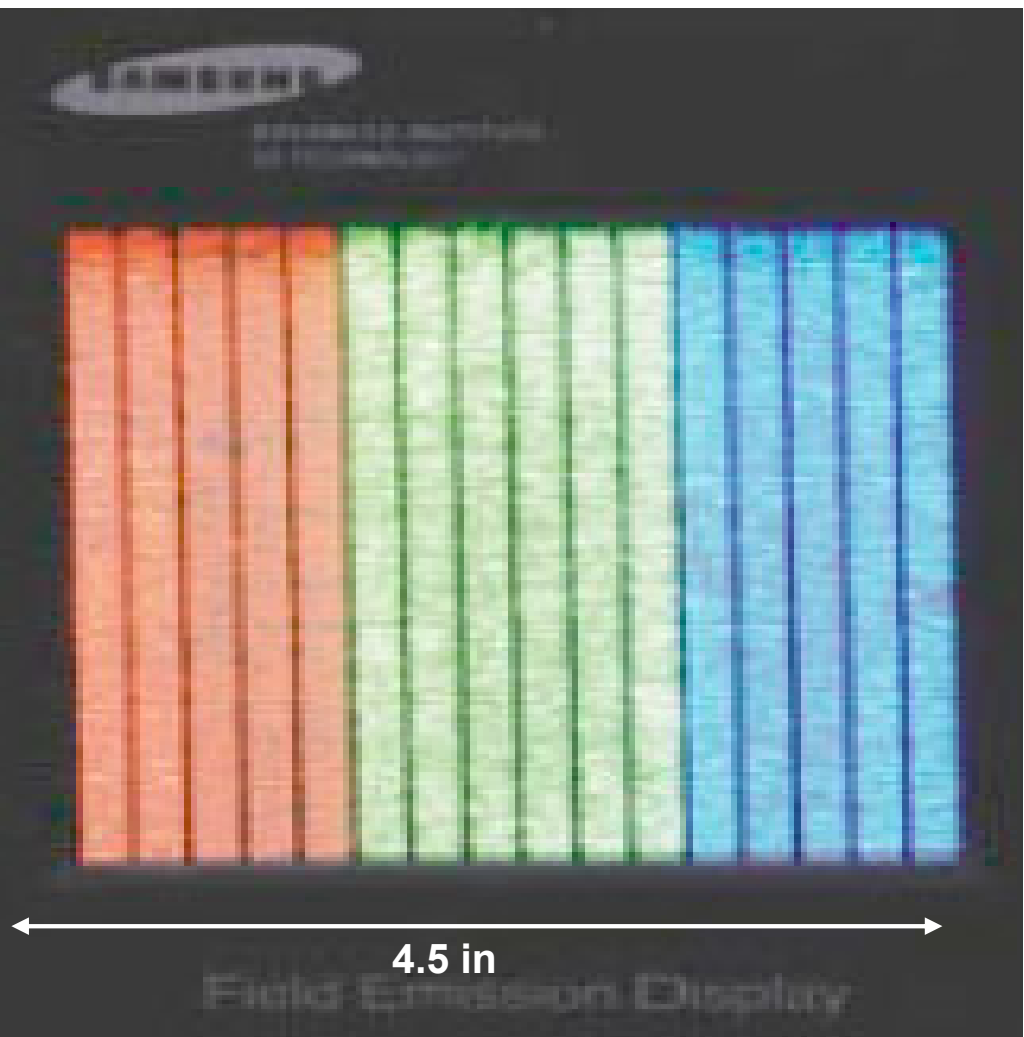


# CNT – Root and Tip Growth





# CNT Field Emission Display

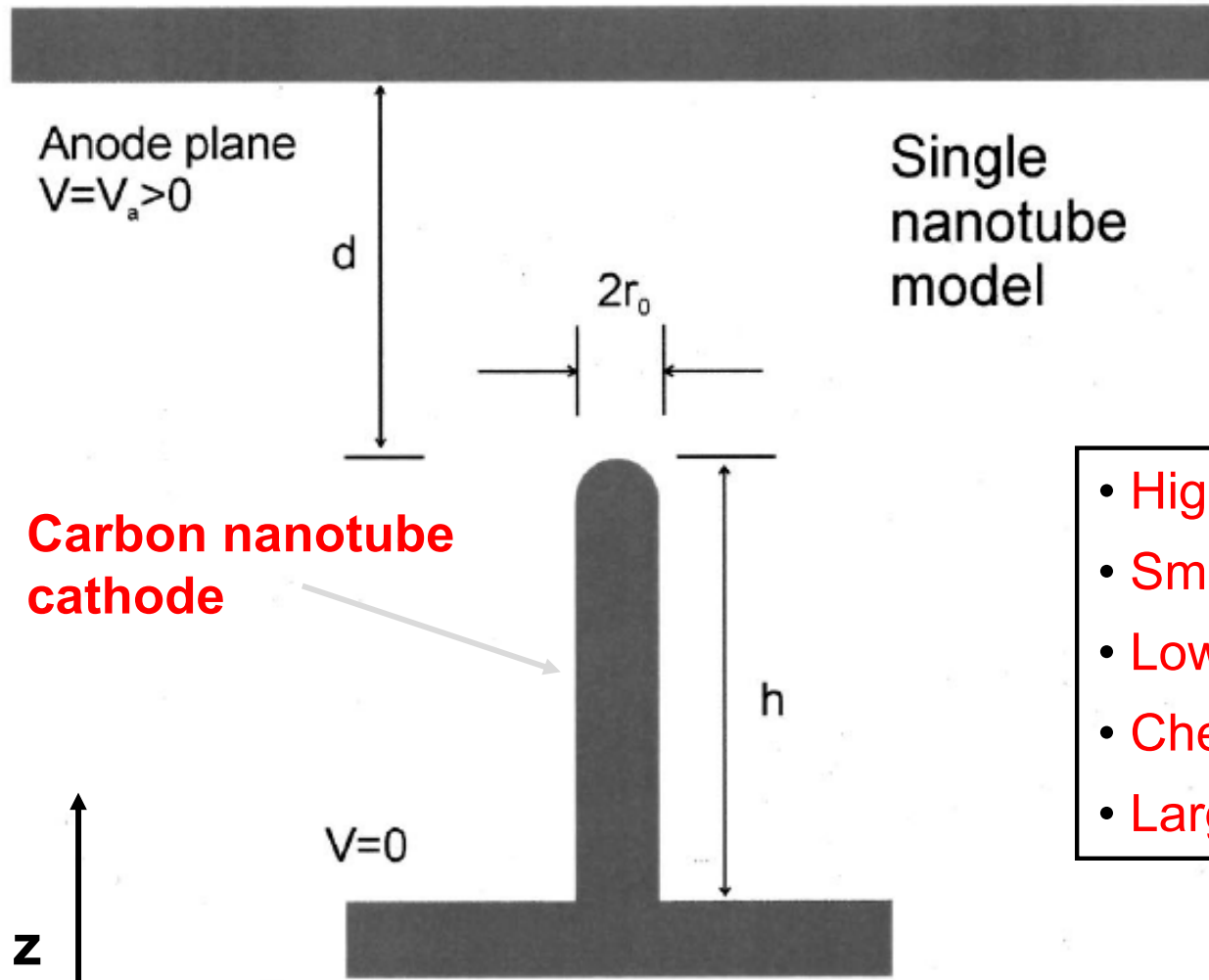


**Carbon nanotube field emission display**  
Samsung Research (Korea)

W.B. Choi et al., *Appl. Phys. Lett.* **75**,  
3129 (1999).



# Field Emission - Carbon Nanotube



**Carbon nanotube cathode**

- High-aspect-ratio emitter
- Small radius of curvature (nm)
- Low extracting fields at CNT tip
- Chemical stability
- Large current density

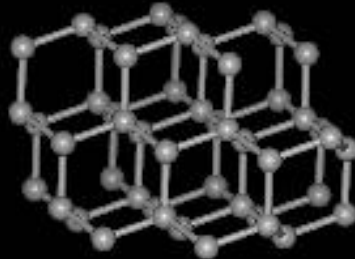
V. Filip, D. Nicolaescu, and F. Okuyama, *J. Vac. Sci. Technol. B* **19**, 1016 (2001)



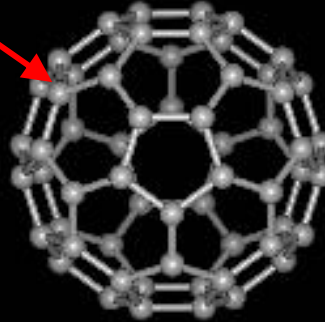


# Various Forms of Carbon

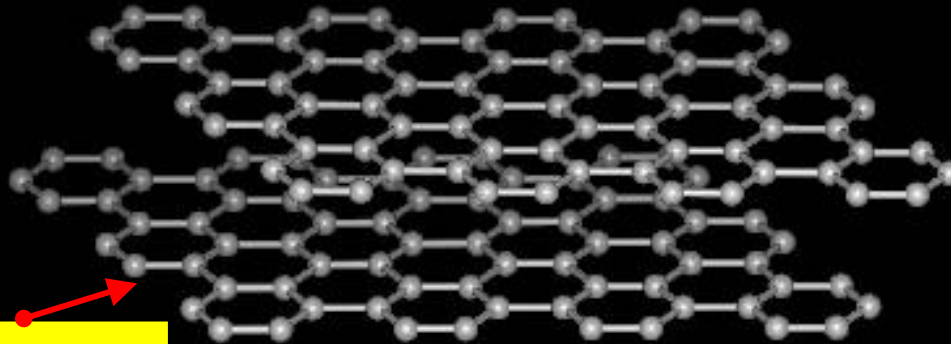
Curl, Kroto, Smalley 1985



diamond

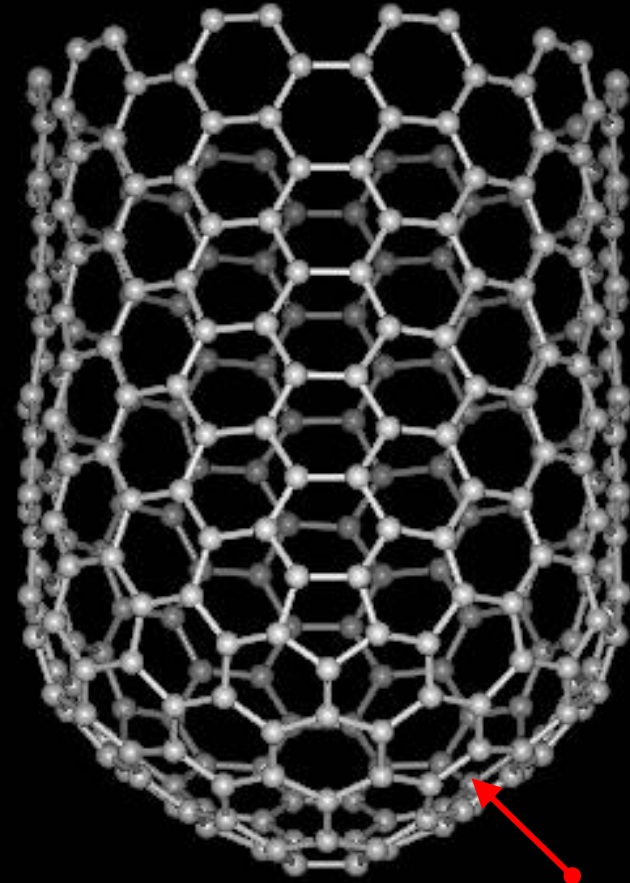


$C_{60}$   
"buckminsterfullerene"



graphite

graphene



(10,10) tube

Iijima 1991

(From R. Smalley's web image gallery)



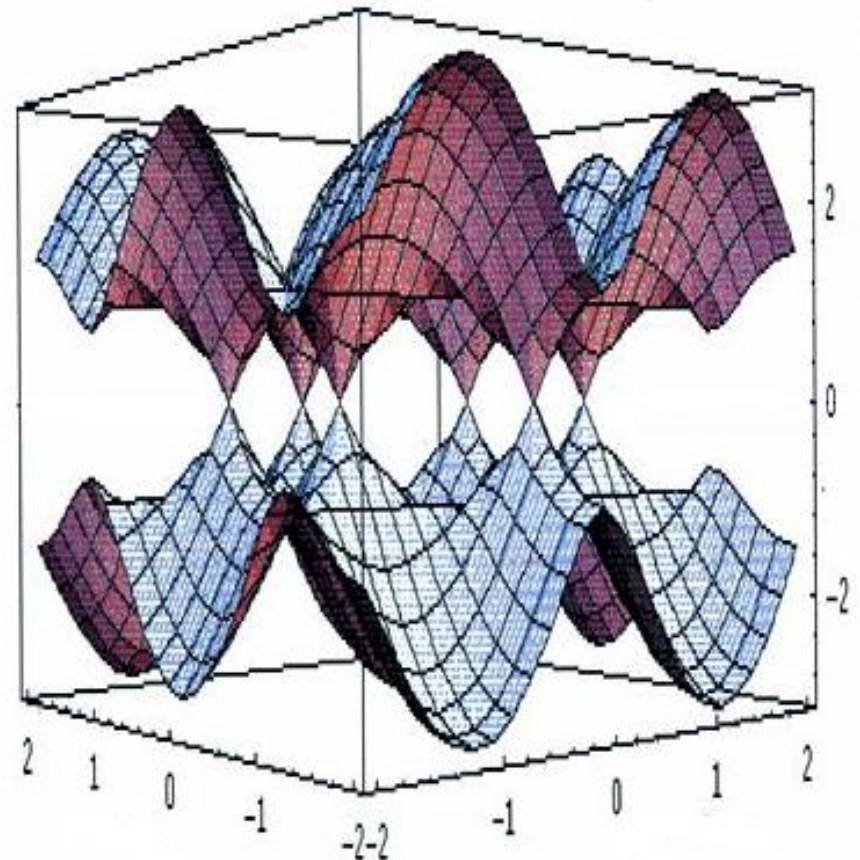
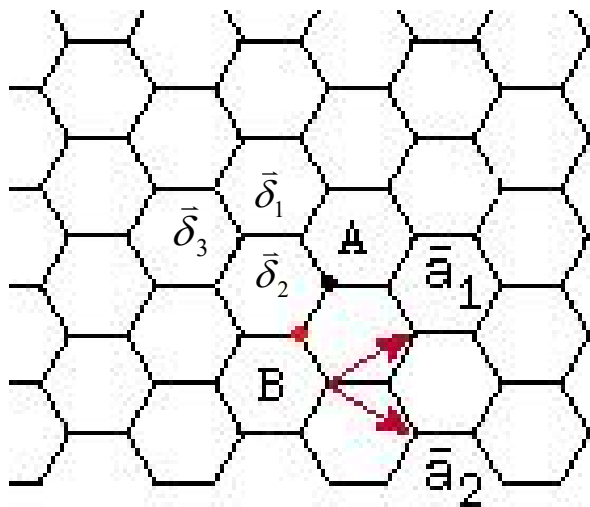
# Why Carbon nanotubes?

- Technological applications
  - **conductive** and **high-strength** composites
  - **energy storage and conversion** devices
  - **sensors, field emission displays**
  - nanometer-sized molecular **electronic devices**
- Basic research: most phenomena of mesoscopic physics observed in CNTs
  - **ballistic**, diffusive and localized regimes in transport
  - disorder-related effects in MWCNTs
  - strong interaction effects in SWCNTs
  - Coulomb blockade and Kondo physics
  - spin transport
  - superconductivity



# Band Structure of Graphene

- Tight-binding model on hexagonal lattice
- Valence and conduction bands touch at  $E=0$

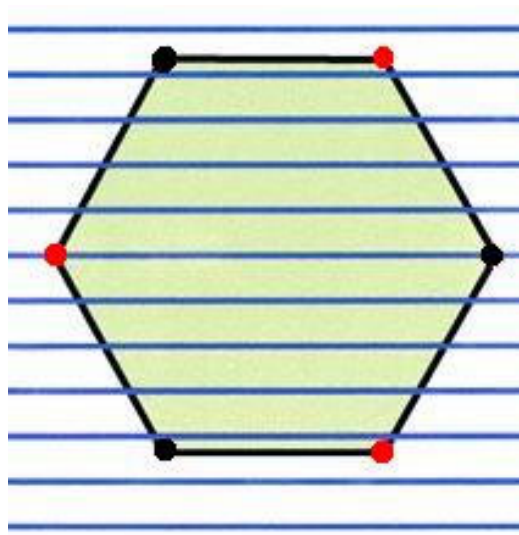




# Electronic Structure of SWNTs

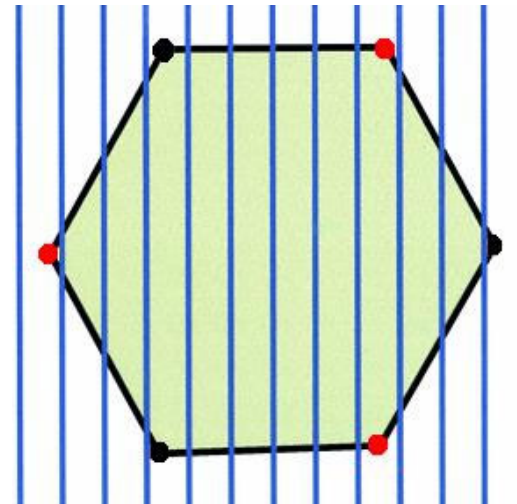
- Periodic boundary conditions →
  - nanotube **metallic** if Fermi points allowed wave vectors, otherwise **semiconducting** !
  - **necessary condition:  $(2n+m)/3 = \text{integer}$**

**armchair**



**metallic**

**zigzag**



**semiconducting**





# Band structure of SWNTs

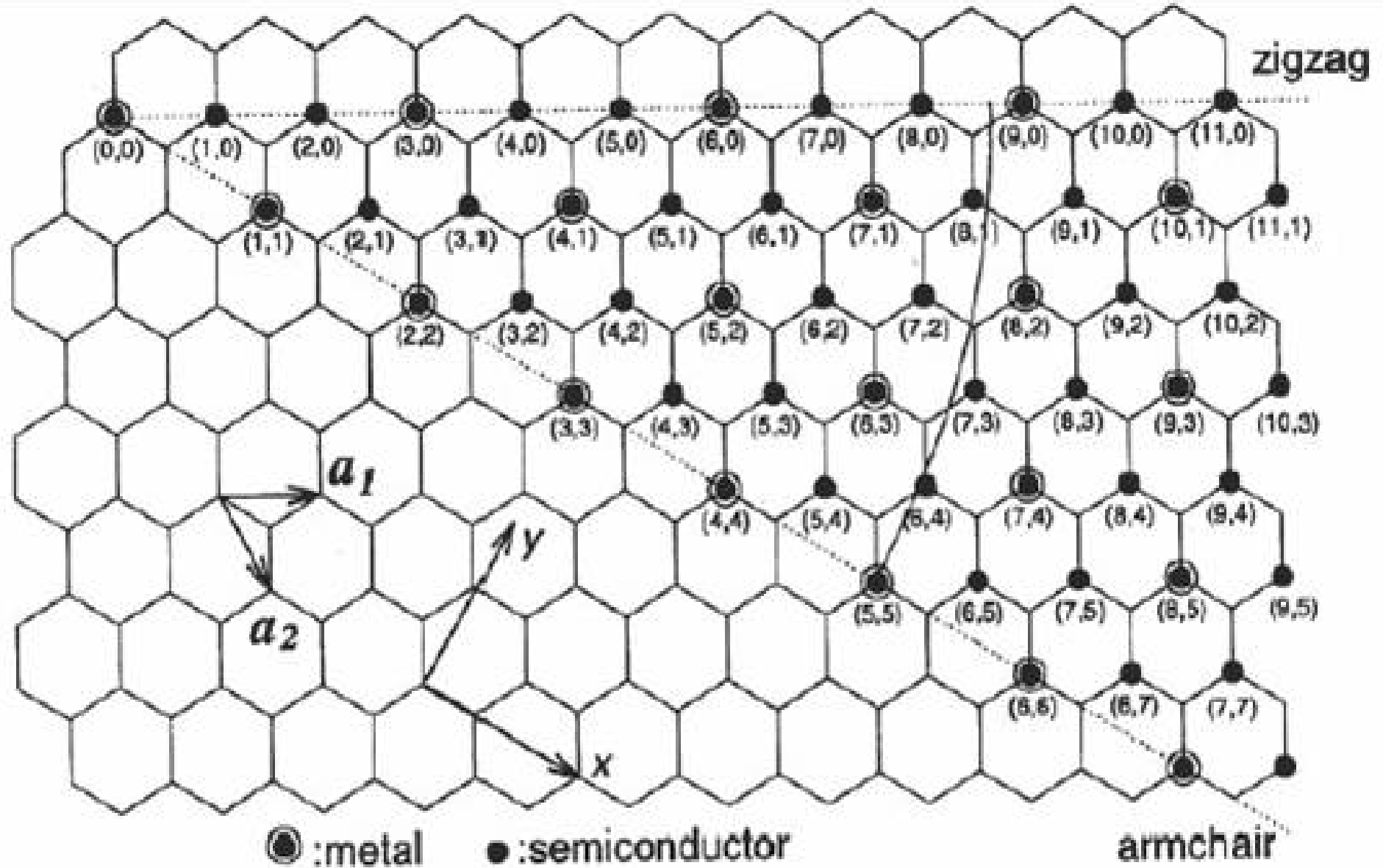
- Band structure predicts three types:
  - **semiconductor** if  $(2n+m)/3$  not integer; band gap:

$$\Delta E = \frac{2\hbar v_F}{3R} \approx 1 \text{ eV}$$

- **metal** if  $n=m$  (armchair nanotubes)
  - **small-gap semiconductor** otherwise (curvature-induced gap)
- Experimentally observed: STM map plus conductance measurement on same SWNT



# Examples





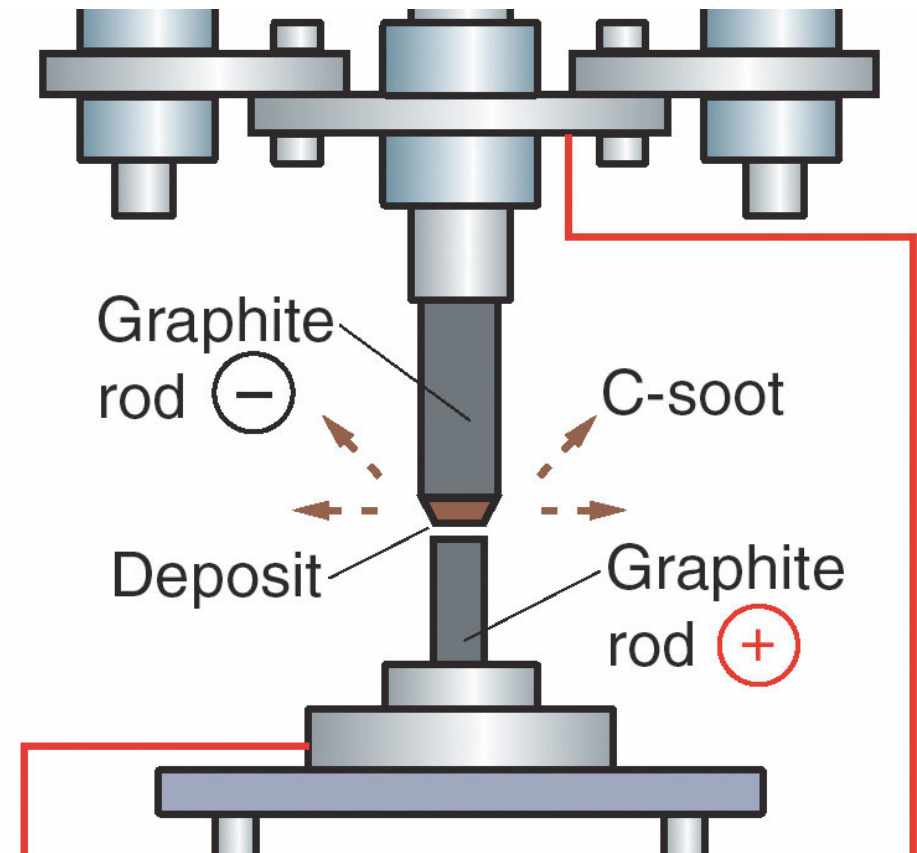
# Synthesis of Nanotubes

- **Carbon arc-discharge**
- **Laser ablation**
- **Chemical vapor deposition**
- Typical sizes
  - 0.4 ~ 3 nm for SWNT (Single-wall nanotube)
  - 1.4~100 nm for MWNT (Multi-wall nanotube)
  - Cost of making, \$750/g for high purity, \$60/g for many impurities!



# Carbon-arc Discharge

- Using high voltages to attract carbon powders
- Yield up to 30%
- Highly depends on environment

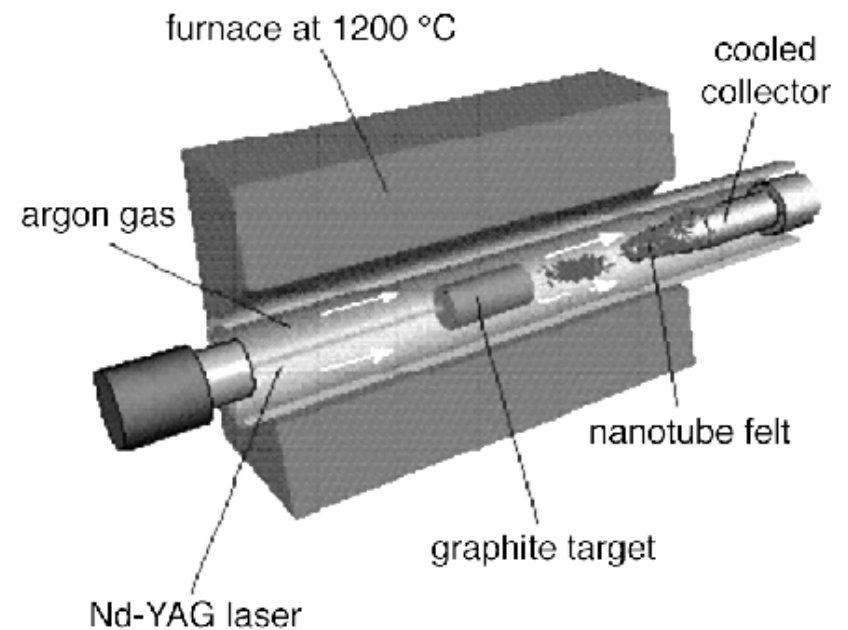


- Image from <http://mrsec.wisc.edu/Edetc/SlideShow/images/nanotubes/arc.jpg>



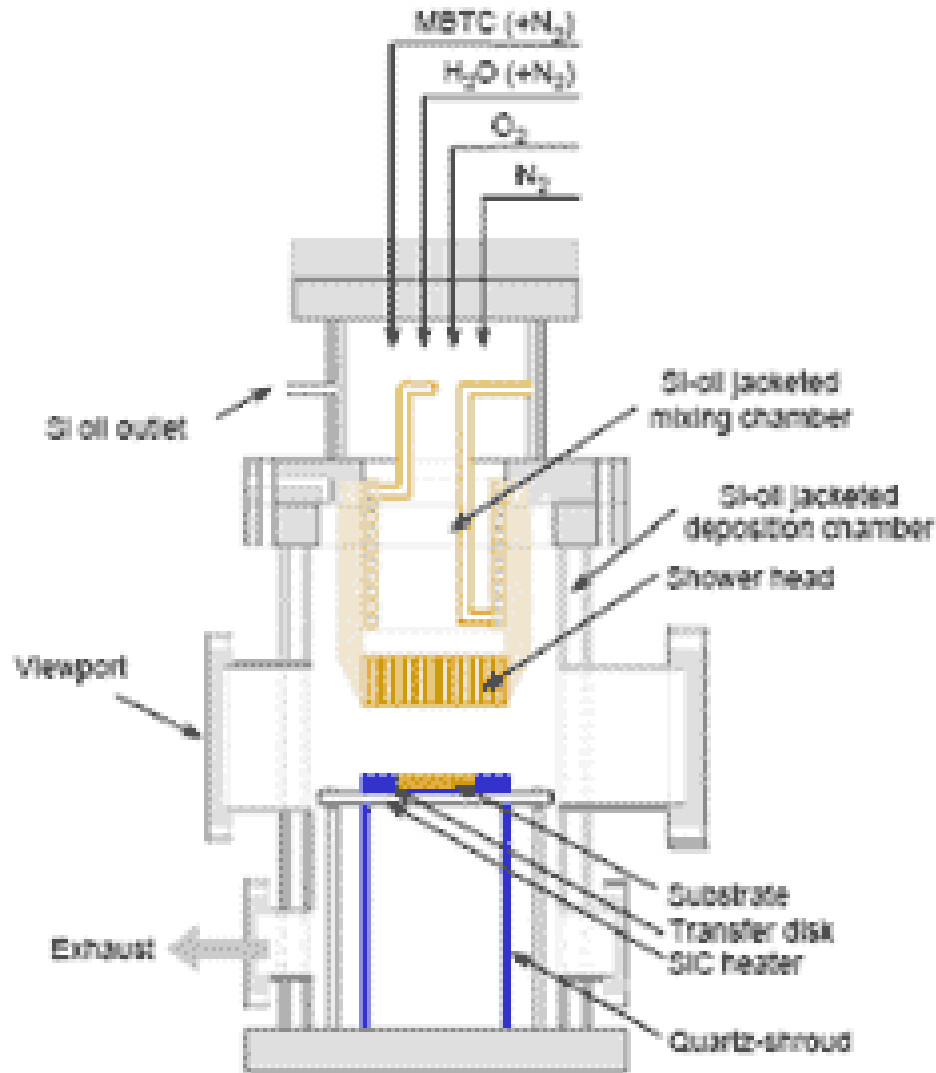
# Laser Ablation

- Pulsing laser and an inert gas in sealed reactor with high temperatures
- Pulsed laser vaporizes graphite
- The graphite vapor condenses forming tubes
- Yield up to 70% by weight
- Very expensive
- Produces SWNT
- Image from [http://ipn2.epfl.ch/CHBU/images/laserva\\_p.gif](http://ipn2.epfl.ch/CHBU/images/laserva_p.gif)





# Chemical Vapor Deposition

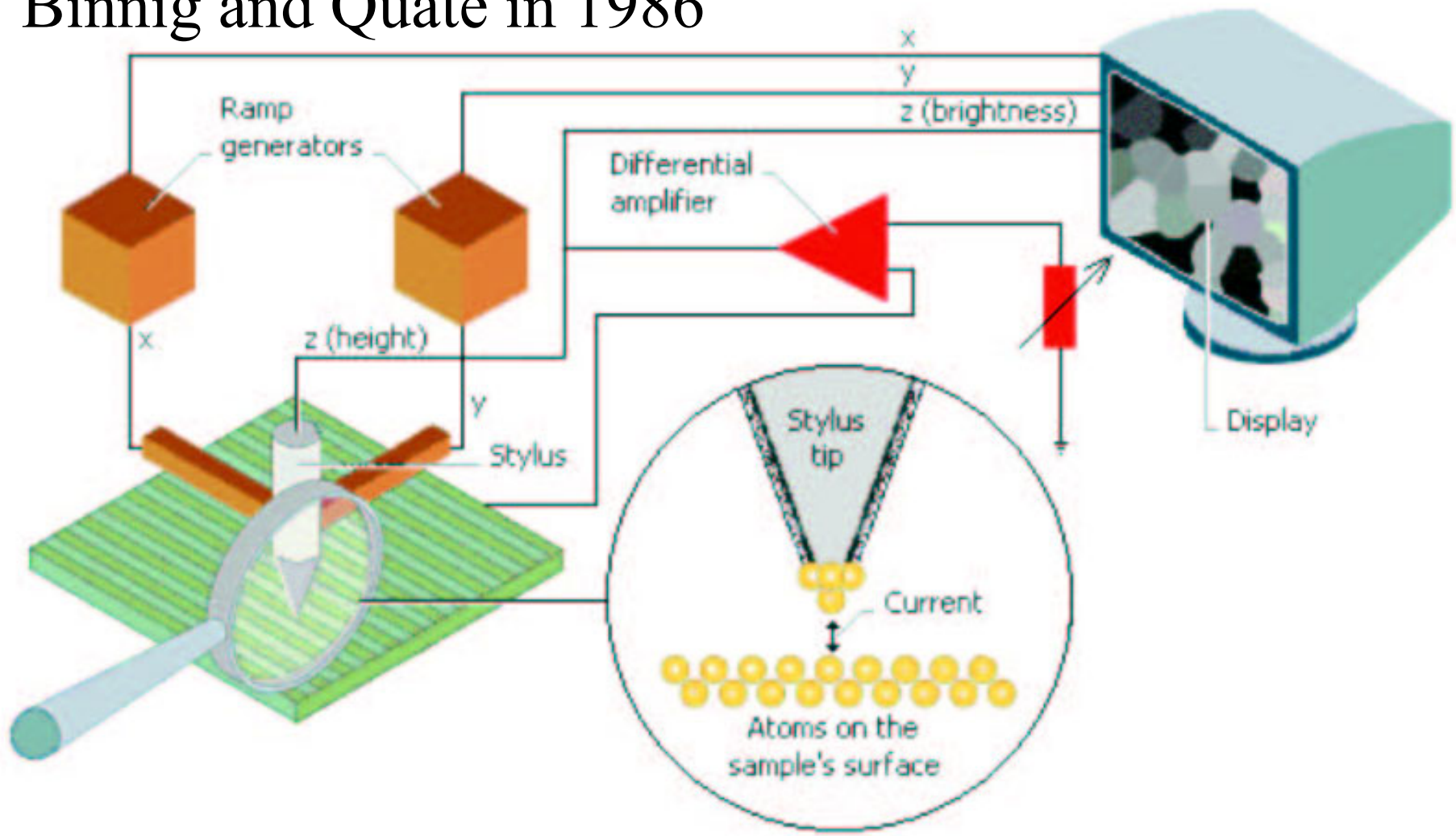


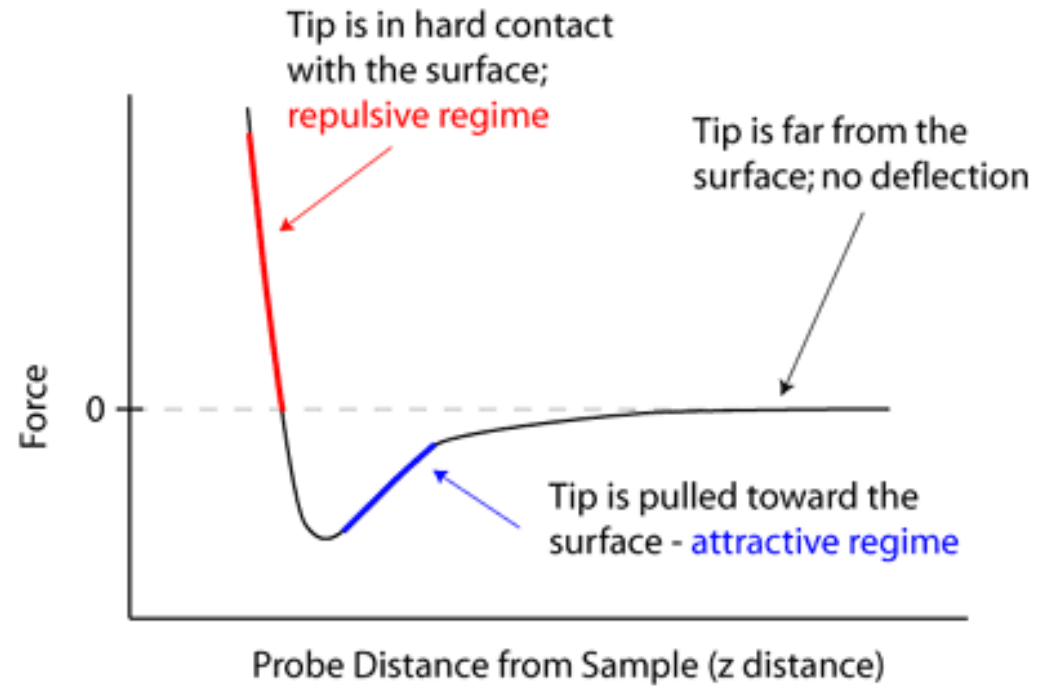
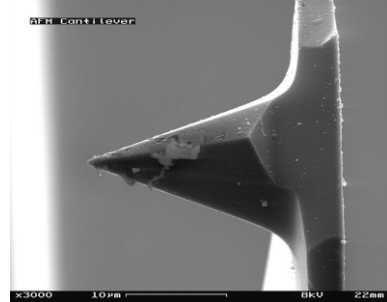
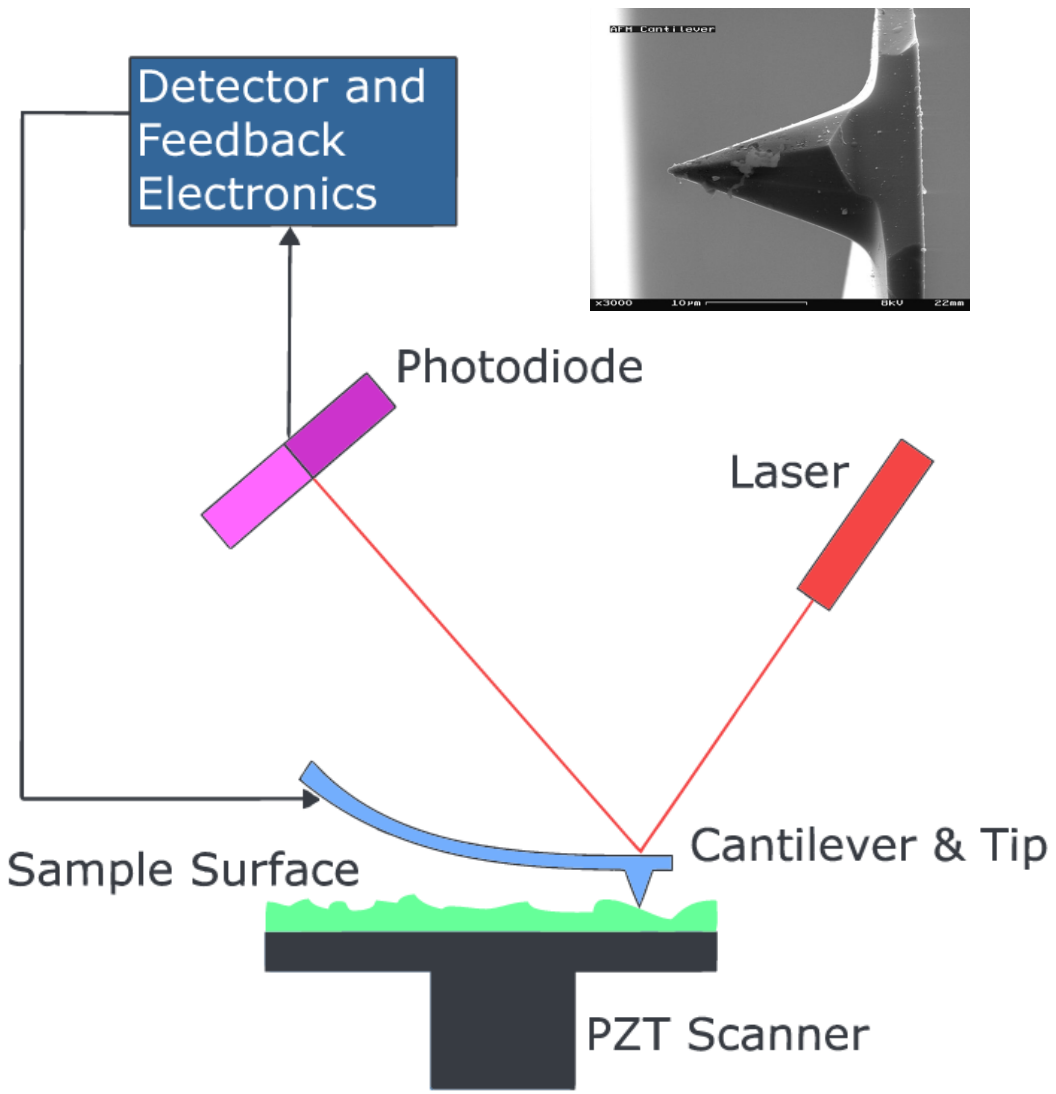
- Substrate made of iron, cobalt, nickel or a combination heated to 700°C
- H<sub>2</sub>, N<sub>2</sub> or NH<sub>3</sub> with CH<sub>4</sub>, C<sub>2</sub>H<sub>5</sub>OH, C<sub>2</sub>H<sub>2</sub> reactor chamber
- Grows at sites where gases meet with substrate
- Process occurs fast
- Potential way of commercially producing nanotubes



# Atomic Force Microscopy

- The **atomic force microscopy** (AFM) was invented by Binnig and Quate in 1986



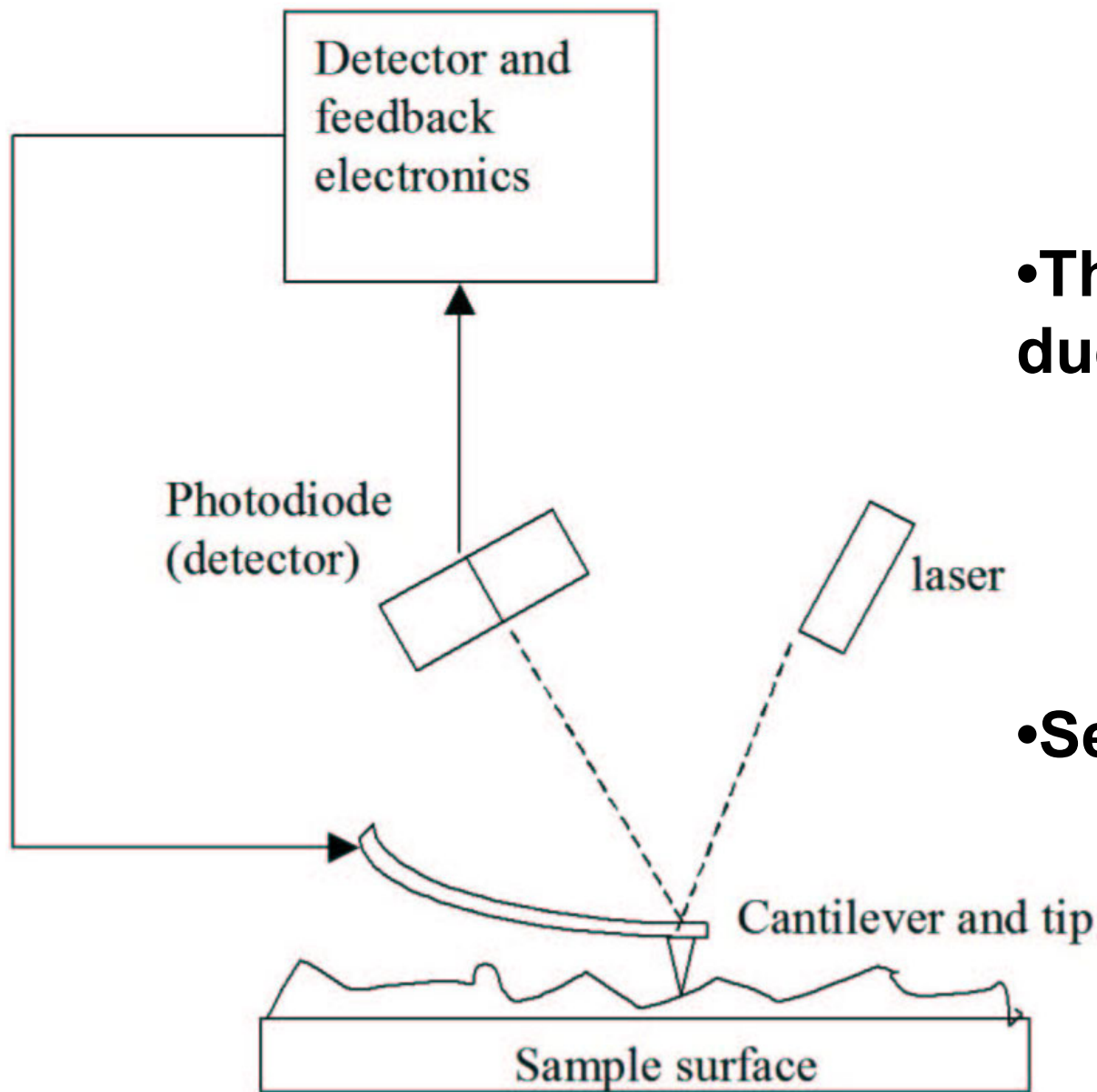


AFM Modes of operation





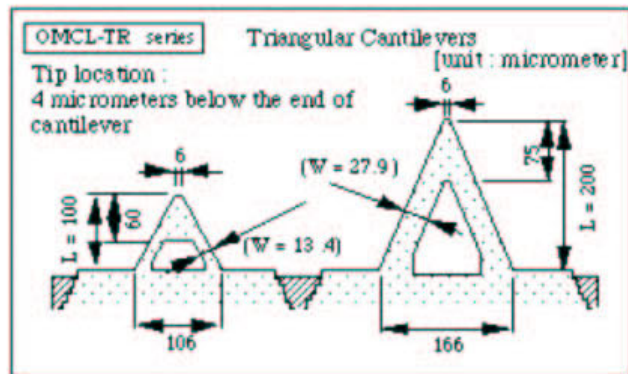
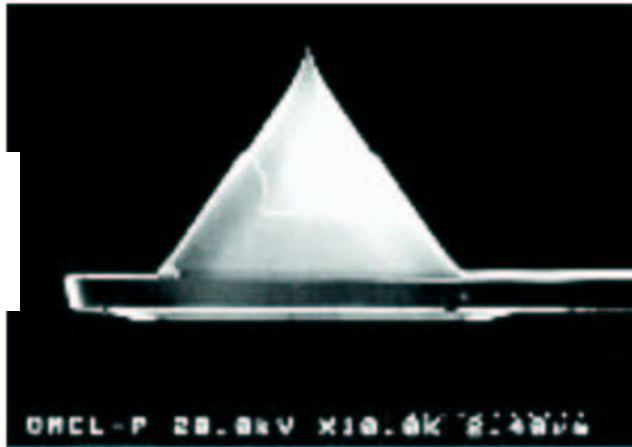
# Schematic of AFM



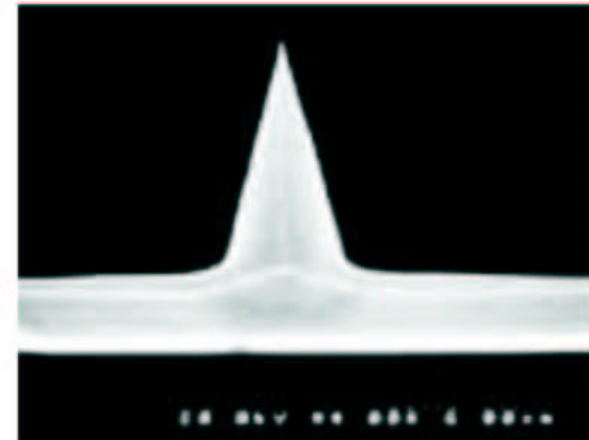
- The AFM detects forces due to
  - van der Waals
  - Electrostatic
  - Magnetic
- Sensitivity limit is 1 aN



# Cantilevers for the AFM



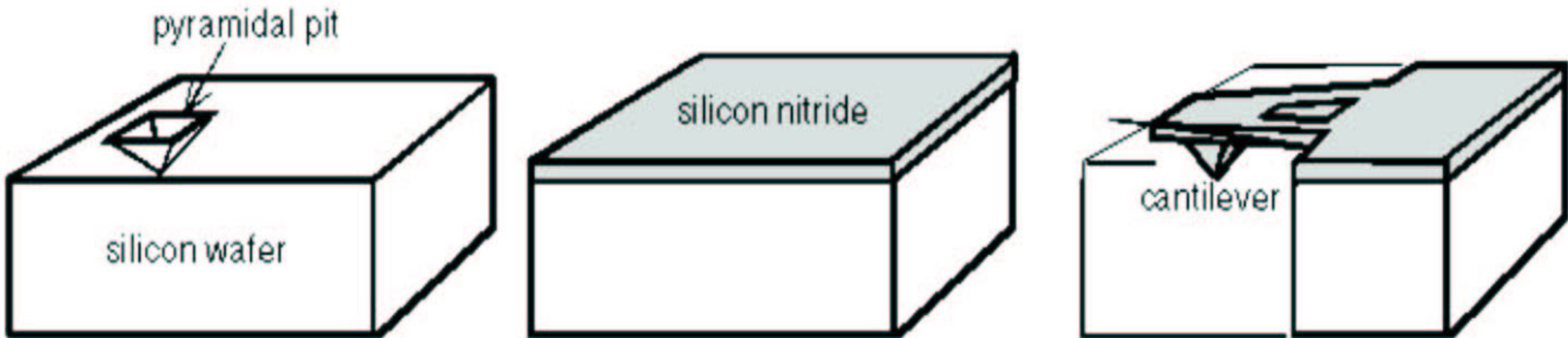
**Silicon Nitride Tip**



**Silicon Tip**

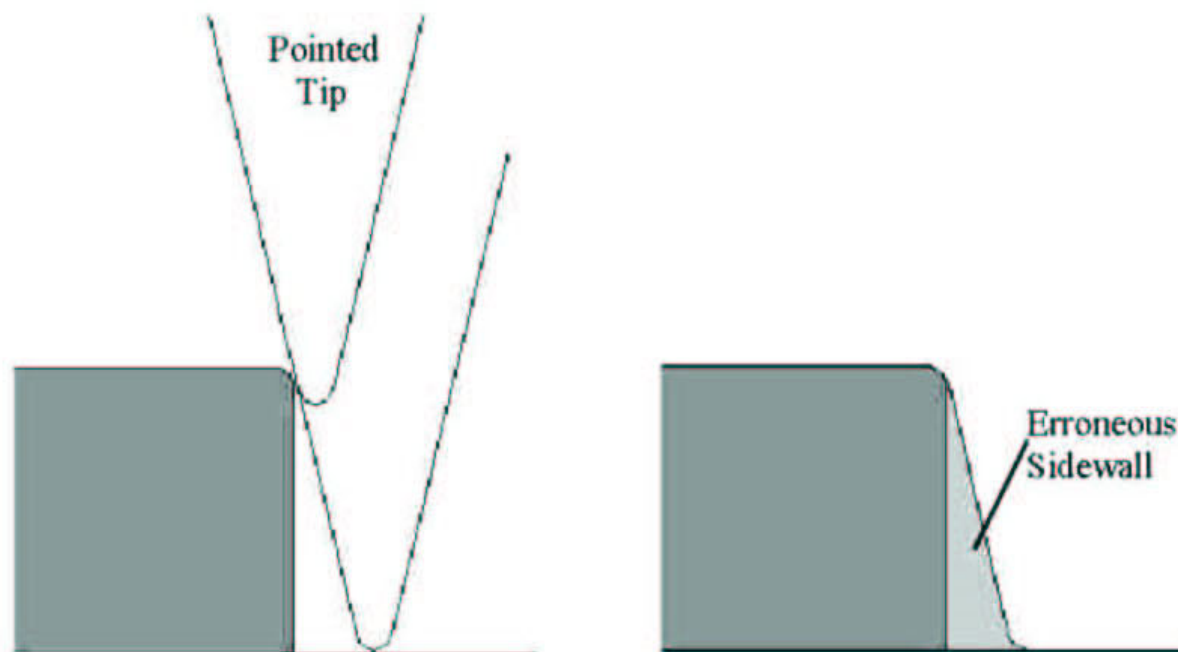


# Silicon Nitride Cantilevers





# How does your tip profile affect your AFM scan?



[http://www.photronics.com/templates/techpapers/bacus\\_manuscript/bacus\\_manuscript4.pdf](http://www.photronics.com/templates/techpapers/bacus_manuscript/bacus_manuscript4.pdf)

# Laser-Induced Graphene Formation

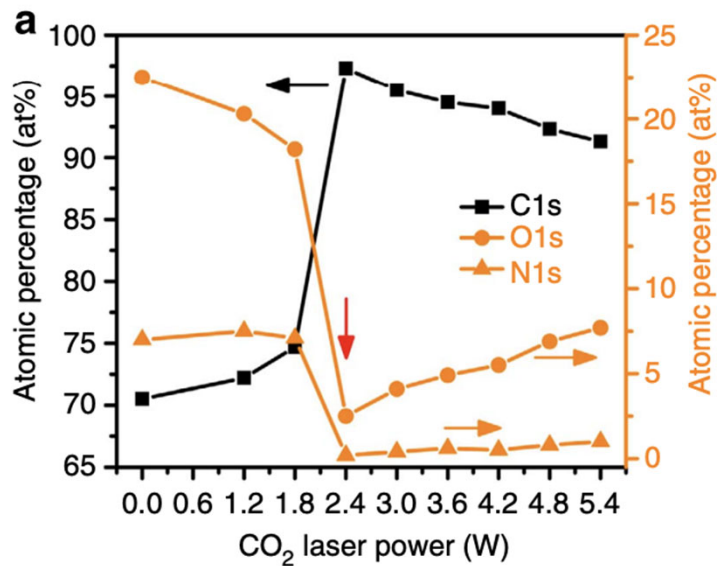


Fig. 3(a) Atomic percentages of carbon, oxygen and nitrogen as a function of laser power. These values are obtained from high-resolution XPS. The threshold power is 2.4W, at which conversion from PI to LIG occurs

- The energy from the laser leads to extremely high localized temperatures ( $> 2500$  °C).
- This high temperature breaks specific bonds (C – O, C = O and N – C bonds) and causes subsequent release of gases.
- Aromatic compounds rearrange to form graphitic structures, with an overlayer of evolved gases minimizing oxidation.
- The mechanism of laser graphitization is linked to structural features in polymer repeat units, especially aromatic and imide units. Only 2 out of 15 tested polymers can form LIG. They both contain aromatic and imide repeat units.

Jason

# In-Plane Interdigitated LIG Microsupercapacitors (LIG-MSCs)

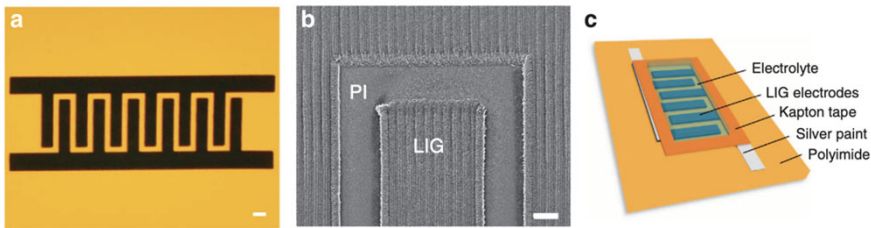


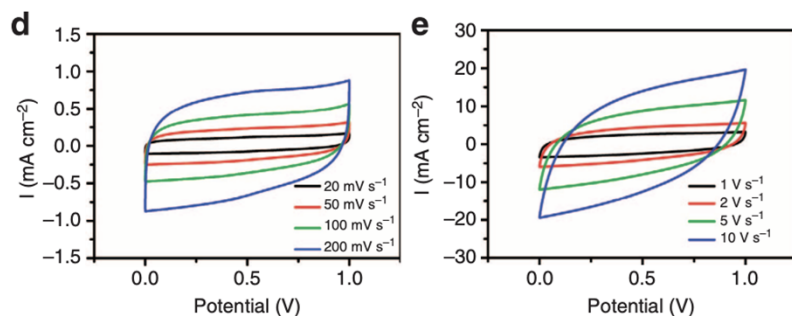
Fig. 4(a) A digital photograph of LIG-MSCs with 12 interdigital electrodes; scale bar, 1 mm.

Fig. 4(b) SEM image of LIG electrodes; scale bar, 200 nm.

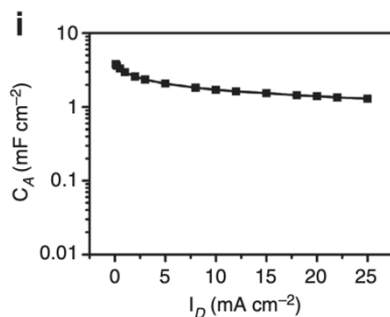
Fig. 4(c) Schematic diagram of LIG-MSCs device architecture.

- LIG serves as both the active electrodes and the current collectors.
- Well-defined LIG-MSC electrodes are directly written on PI sheets with a neighbouring distance of 300  $\mu\text{m}$
- Silver paint was applied on common positive and negative electrodes.
- Kapton tape was employed to define the active electrodes.

# Electrochemical Performance



4(d & e) CV curves of LIG-MSCs at scan rates from 20 to 10000 mVs<sup>-1</sup>



4(f) Specific areal capacitance ( $C_A$ ) calculated from CV curves as a function of scan rates

- Cyclic voltammetry (CV) and galvanostatic charge – discharge (CC) measurements were performed to investigate the electrochemical performance of the fabricated LIG-MSCs
- Good double-layer capacitive behaviours are shown from the CV curves.
- LIG-MSCs constructed with LIG-4.8 W electrodes exhibit the highest specific areal capacitance.
- All other electrochemical measurements were carried out on LIG-MSCs made from PI with a laser power of 4.8 W.

Jason

# Electrochemical Performance

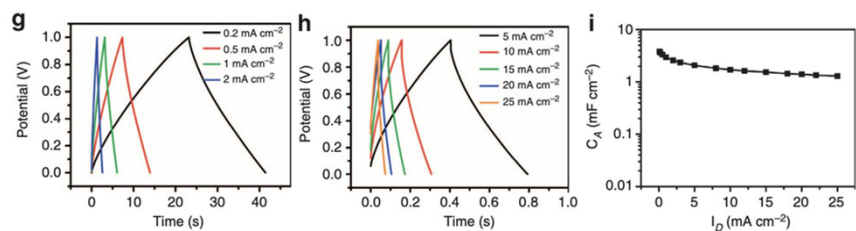


Fig. 4(g & h) CC curves of LIG-MSCs at discharge current densities ( $I_D$ ) varied from 0.2 to 25 mA cm<sup>-2</sup>.

Fig. (I),  $C_A$  calculated from CC curves versus  $I_D$

- After comparing capacitance with GO-derived supercapacitors and carbon-based MSCs, LIG-MSCs show excellent capacitive behaviour.
- A low equivalent series resistance of 7  $\Omega$  suggests good conductivity and rapid charge-discharge capabilities.



# Electrochemical Performance

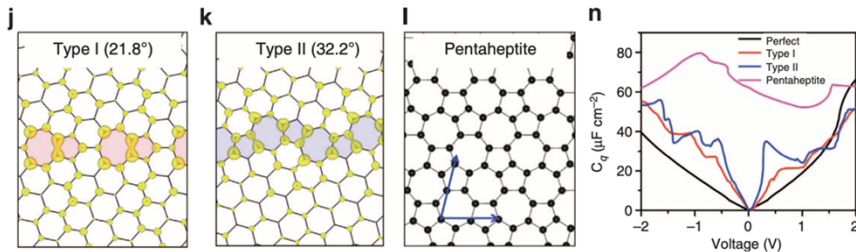


Fig. (j and k), Charge density distribution of the states within a voltage window (-0.1, 0.1) V for type I and II polycrystalline sheets. The defects at the grain boundaries are shadowed, and numbers show the misorientation angle between the grains.

Fig. (l) A carbon layer fully composed of pentagons and heptagons (pentaheptite).

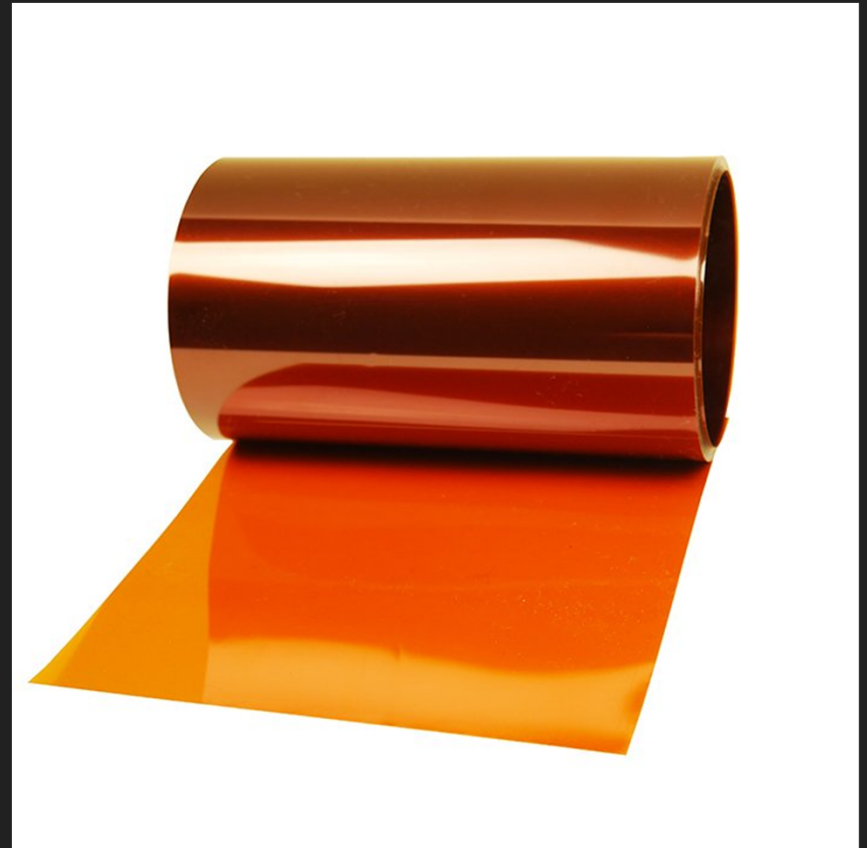
Fig. (n) Calculated quantum capacitance (defined in the text) of perfect and polycrystalline/disordered graphene layers.

- LIG-MSCs offer more energy or power density or both.
- When compared with recently demonstrated reduced GO-film, MSCs (MPG-MSCs), and laser-scribed graphene MSCs (LSG-MSCs), LIG-MSCs can deliver comparable  $E_V$ , although power performance needs to be enhanced.
- LIG-MSCs exhibit 100 times higher areal energies  $E_A$  and 4 times power densities  $P_A$  than MPG-MSCs.
- LIG-MSCs offer slightly better  $E_A$  than LSG-MSCs with comparable power performance.

# Methods

## Experimental Setup

- Utilized Kapton Polyimide film and various polymer sheets from McMaster-Carr
- CO2 laser cutter system (Universal X-660) with 10.6 mm wavelength and 14 ms pulse duration employed for laser scribing.
- Laser power varied from 2.4 to 5.4W with 0.6W increments; fixed scan rate of 3.5 inches/s and 1,000 pulses per inch.



# Methods

## Methodological Parameters

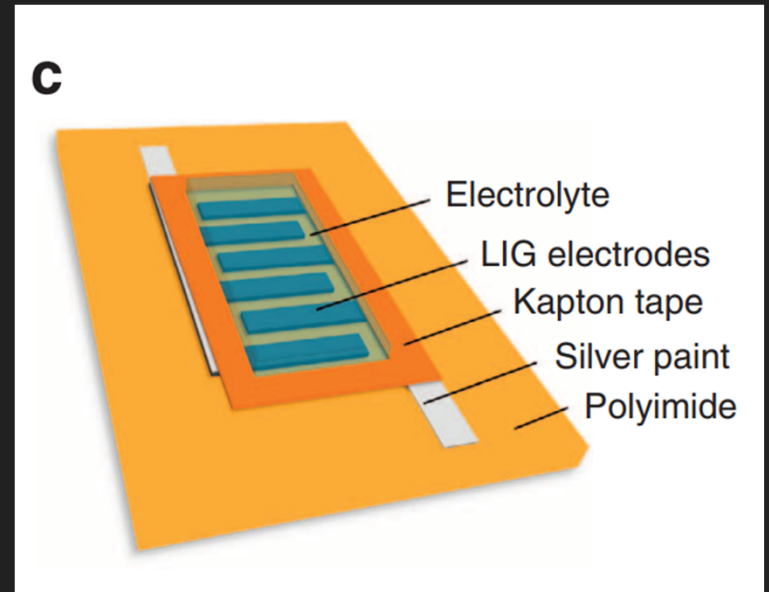
- Laser system options included adjustable scan rates (0.7 to 23.1 inches/s) and p.p.i. settings (10–1,000 p.p.i.).
- Experimentation revealed pulses per inch (ppi) had minimal impact on changing threshold power.
- All laser experiments conducted under ambient conditions had consistent scan rate (3.5 inches/s) and 1,000 p.p.i. was used for all experiments unless specified otherwise.



# Methods

## Device Fabrication Overview

- CO<sub>2</sub> laser used for direct writing of LIG electrodes.
- Laser-Induced Graphene serves as active electrodes and current collectors in microsupercapacitors.
- Silver paint enhances electrical connectivity; Kapton PI tape protects contact pads in the meshed area.



# Methods

## Characterization

- SEM images were taken on a FEI Quanta 400 high resolution field emission instrument.
- The TEM and high-resolution TEM were performed using a 2,100 F field emission gun.
- Aberration-corrected scanning TEM images were taken using an 80 kiloelectron volt Japan Electron Optics Laboratory ARM200F equipped with a spherical aberration corrector.



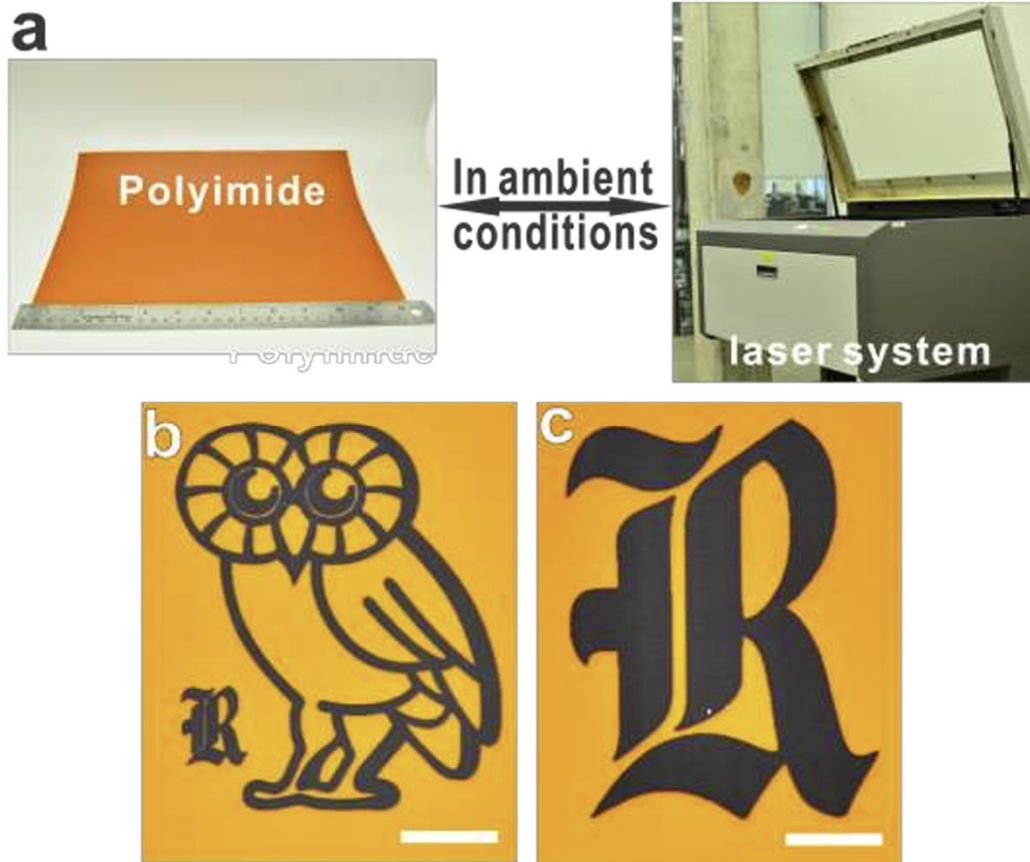
# Methods

## Measurements

- CV, galvanostatic CC measurements, and electrical impedance testing performed using a CHI 608D workstation.
- All measurements conducted in ambient conditions.
- The experimental focus extended to include aqueous electrolytes.



## Materials and equipment for production of LIG from PI by laser scribing

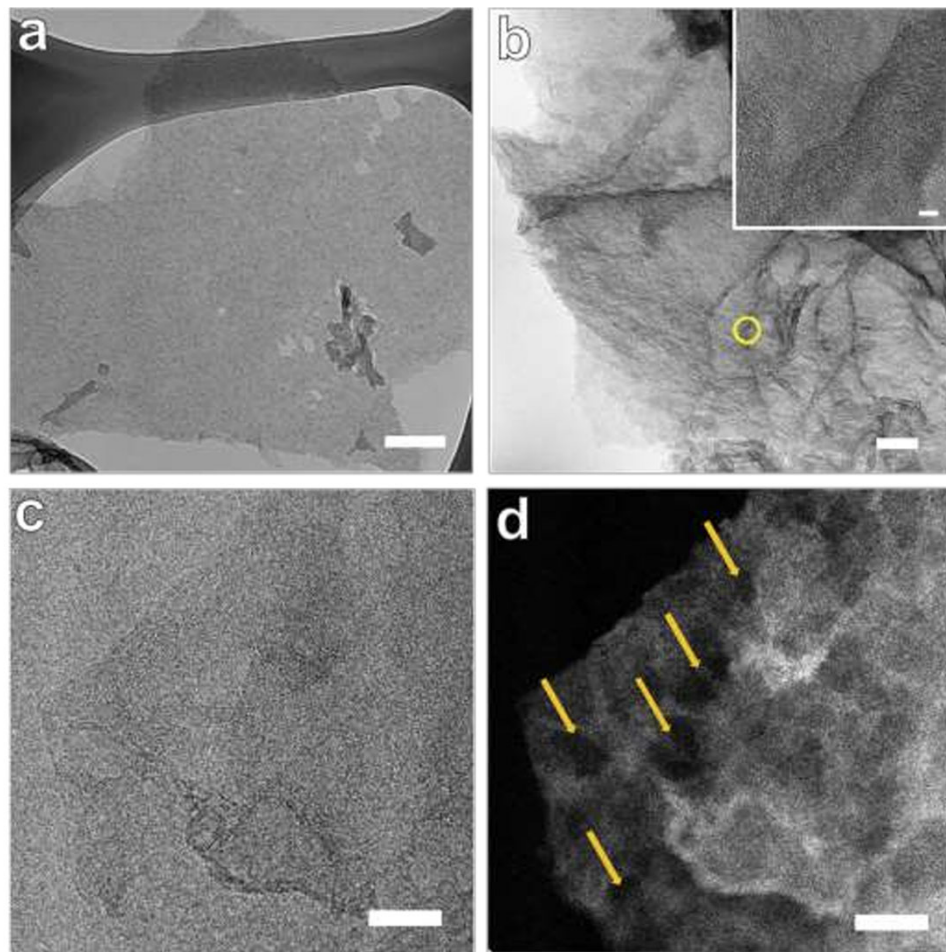


- Photographs of commercial Kapton PI sheets with a 30 cm ruler on the left, and the laser cutting system on the right
- Photograph of an owl patterned on a PI substrate;
- Photograph a letter R patterned on a PI substrate;



# Transmission Electron Microscopy (TEM) Characteristics of LIG-3.6 w Flakes

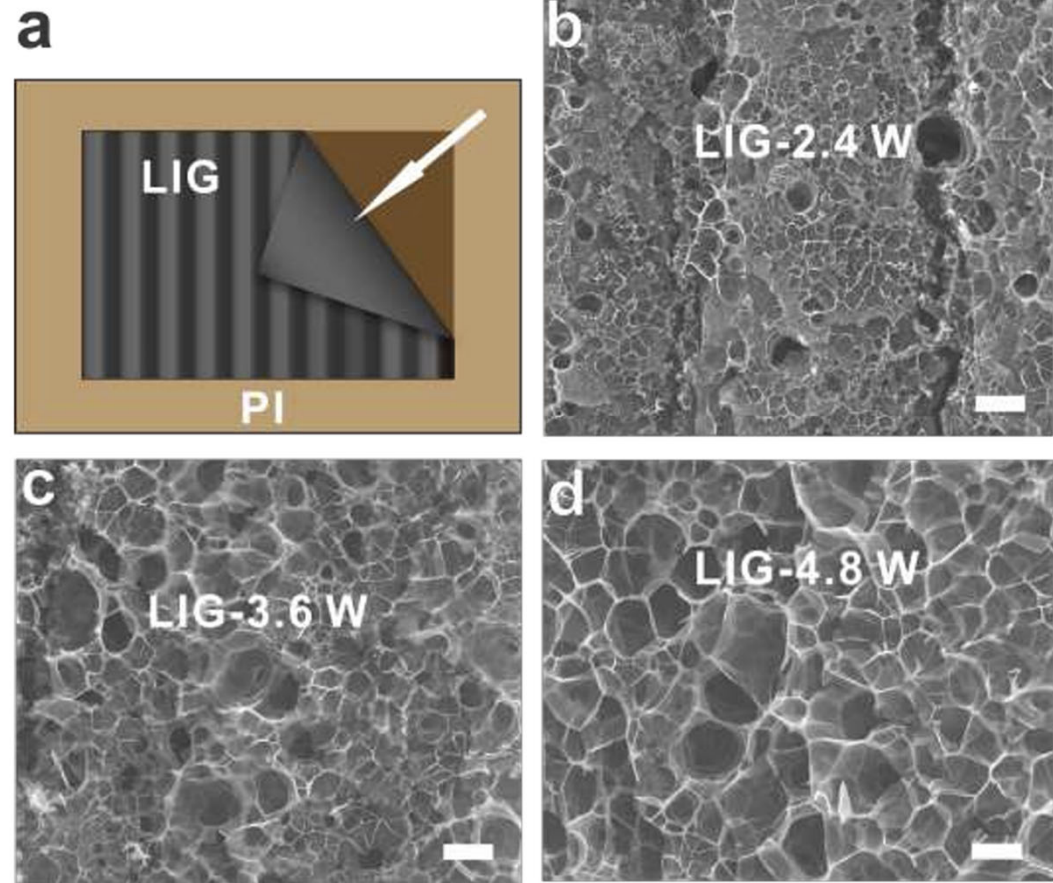
- a) TEM image of a thin LIG flake atop a carbon grid; scale bar 200 nm
- b) TEM image of a thick LIG flake showing entangled tree-like ripples; scale bar 100 nm
- c) TEM image of LIG in bright field view; scale bar 10 nm
- d) TEM image of LIG in dark field view; scale bar 10 nm





## Characterizations of backsides of LIG films

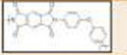
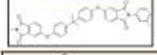
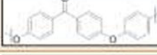

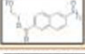





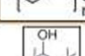

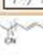
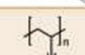
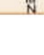
- a) Scheme of the backsides of LIG films peeled from PI substrates.
- b) SEM images of backsides of LIG films obtained at laser powers of b) 2.4 W; c) 3.6 W; and d) 4.8 W; Scale bars are 10 nm



# Supplementary Tables

Summary of polymers, their chemical repeat units and their LIG forming capability. Out of 15 polymers, only PI and PEI were successfully converted to LIG.

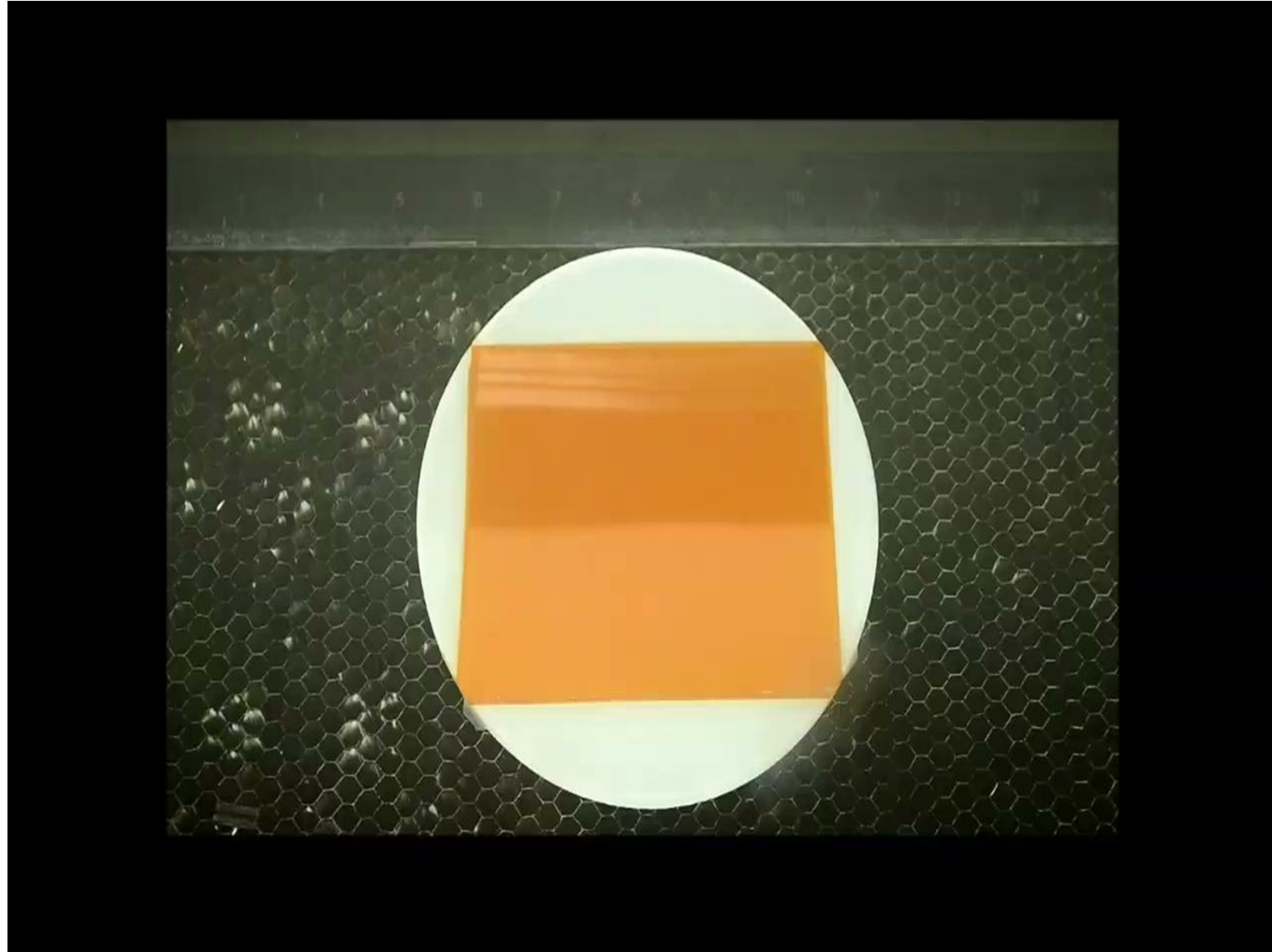
Materials	Carbon (%)	Oxygen (%)	Nitrogen (%)
<b>Polyimide</b>	<b>70.5</b>	<b>22.5</b>	<b>7.0</b>
LIG-1.2 W	72.2	20.3	7.5
LIG-1.8 W	74.7	18.2	7.1
LIG-2.4 W	97.3	2.5	0.2
LIG-3.0 W	95.5	4.1	0.4
LIG-3.6 W	94.5	4.9	0.6
LIG-4.2 W	94.0	5.5	0.5
LIG-4.8 W	92.3	6.9	0.8
LIG-5.4 W	91.3	7.7	1.0

Full Name	Symbols	Unit	Graphitized?
Kapton Polyimide	PI		Yes
Ulse Polyetherimide	PEI		Yes
Polyether ether ketone	PEEK		No
Polyethylene terephthalate	PET		No
Polyethylene naphthalate	PEN		No
Fluorinated ethylene propylene	FEP		No
Perfluoroalkoxy alkanes	PFA		No
Teflon	PTFE		No
Polystyrene	PS		No
Polycarbonate	PC		No
Polyethylene	PE		No
Polyvinyl alcohol	PVA		No
Poly(methyl methacrylate)	PMMA		No
Acrylonitrile butadiene styrene	ABS		No
Poly(acrylonitrile)	PAN		No

Summary of atomic percentage of elements in raw material (PI) and LIG derived from different laser powers.

## Fabrication process of LIG microsupercapacitor

It took ~15 min to fabricate these devices with  $\sim 7\text{ cm} \times \sim 6\text{ cm}$  area. This movie shows that this technology in fabricating in-plane supercapacitors can be easily scaled.



# References

1. Lin, J., Peng, Z., Liu, Y., Ruiz-Zepeda, F., Ye, R., Samuel, E. L. G., Yacamán, M. J., Yakobson, B. I., & Tour, J. M. (2014). Laser-induced porous graphene films from commercial polymers. *Nature Communications*, 5(1). <https://doi.org/10.1038/ncomms6714>
2. Ma, J., Alfe, D., Michaelides, A. & Wang, E. Stone-Wales defects in graphene and other planar sp(2)-bonded materials. *Phys. Rev. B* 80 (2009).
3. El-Kady, M. F. & Kaner, R. B. Scalable fabrication of high-power graphene micro supercapacitors for flexible and on-chip energy storage. *Nat. Commun.* 4, 1475 (2013).
4. Wu, Z. S., Parvez, K., Feng, X. L. & Mullen, K. Graphene-based in-plane micro supercapacitors with high power and energy densities. *Nat. Commun.* 4, 2487 (2013).





# Lab #1

## Lab 1 (Direct-write Laser Conversion of Graphene)

Please read through paper #2 carefully as lab #1 is based on the same process. TA will prepare the polymer samples and provide some guidelines for the operation of the laser setup.

- (1) Go to 1113 Etcheverry at the time you are assigned and take a photo of the specimen you are assigned before the synthesis process. You should ask TA or reader on the specific dimensions, thickness ... of the specimen
- (2) Under the guidance of TA or Reader, please place the sample into the laser setup and set the right parameters similar to paper #2 with a target synthesize graphene as suggested by TA or Reader.
- (3) After the synthesis process, please move the sample out of the setup. Please take a photo for the sample after the synthesis process
- (4) Measure the IV response of graphene
- (5) Estimate the resistance of the graphene and if possible, suggest ways to measure the contact resistances.
- (6) write a short (1 page) report about this lab, including IV response of graphene.
- (7) EXTRA POINTS: If you are interested in this lab, you can design and program your own patterns for specific purpose/application

# Electrothermal Carbon Nanotube Gas Sensor

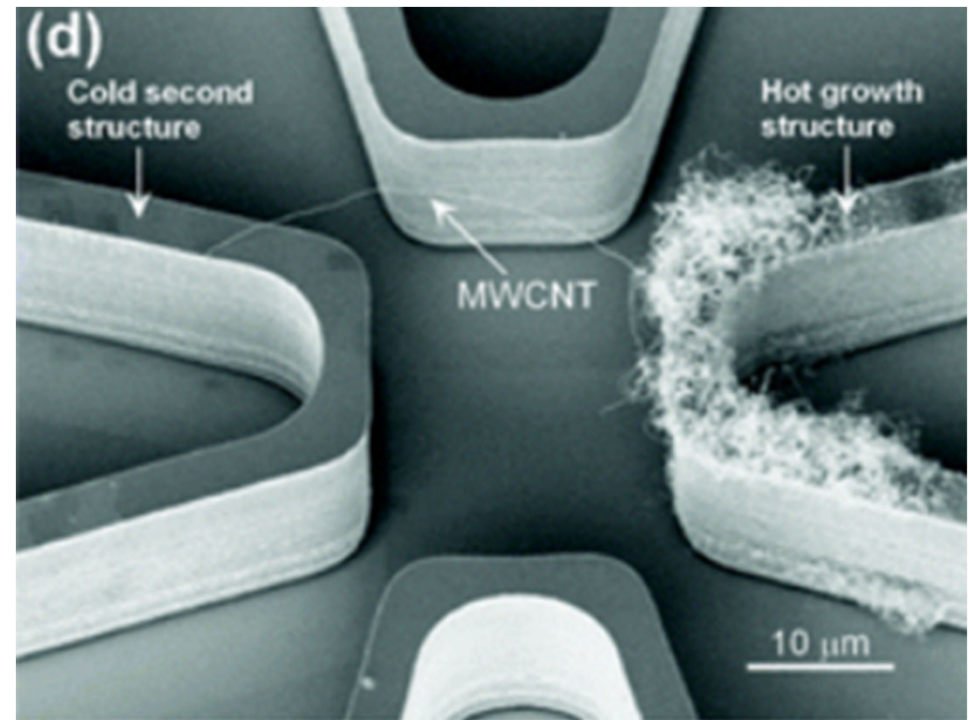
Takeshi Kawano, Heather C. Chiamori, Marcel Suter, Qin Zhou, Brian D. Sosnowchik,  
and Liwei Lin

*Nano Lett.* 2007, 7, 12, 3686–3690

Publication Date: November 15, 2007

# Introduction

- Investigate the electrothermal effect of a single **multi walled carbon nanotube (MWCNT)**
- **Limiting factors** include low adsorption energies, diffusion kinetics, response speed, selectivity, and reversibility
- **MWCNT is grown** on silicon using a local synthesis method and accomplished in less than a minute





# Operation

- **MWCNT is suspended** between two silicon microstructures and is heated by electrical current
- **Each successful connection** between a CNT and the connecting microstructures is shown by a voltage spike in figure 1 b and 1 c
- The **MWCNT experiences temperature and resistance changes** based on the heat-transfer with surrounding gas
- **All data** is from MWCNT shown in figure 1 d

